Electronic Supplementary Material (ESI) for Energy & Environmental Science.
This journal is © The Royal Society of Chemistry 2017

Electronic Supplementary Information

Degradation-induced Capacitance: A New Insight into the Superior Capacitive Performance of Polyaniline/Graphene Composites

Qin'e Zhang,[a] An'an Zhou,[a] Jingjing Wang,[a] Jifeng Wu[a] and Hua Bai*[ab]

a College of Materials, Xiamen University, Xiamen, 361005, China, P.R.

b Graphene Industry and Engineering Research Institute, Xiamen University, 361005, China, P. R.

E-mail: baihua@xmu.edu.cn

Calculation of theoretical specific capacitance of PANI/RGO and HAOANIs

For electroactive polymers and oligomers, the theoretical specific capacitance (C_T) can be predicted by the following equation.[1, 2]

$$C_T = \frac{nF}{\Delta EM}$$

Where n is the average number of electrons transferred during the redox reaction, F is the Faraday constant (= 96485 C mol^{-1}), M is the molecular mass of monomer, ΔE is the potential range. The theoretical capacitance value of ~ 740 F g^{-1} is obtained[2] in the potential range of −0.2 ~ 0.8 V (or 0 ~ 0.8 V) for PANI. Theoretical gravimetric capacitance of graphene[3, 4] is about 550 F g^{-1}, but the practical specific capacitance[4, 5] of RGO is approximately 220 F g^{-1}. If we assume that the surface area of PANI/RGO composite equals to that of RGO component in the composite, and that the areal specific capacitance of PANI is the same as that of RGO, the theoretical capacitance of PANI/graphene composites (PANI content: a), which is about

$$C_T = 740a + 220 \times (1 - a)$$

Therefore, we can simply calculate the theoretical capacitance of PANI/graphene composites and hydroxyl or amino terminated oligoanilines (HAOANIs) appearing below.

a) Flexible graphene/PANI paper (PANI content: 22.3%):[6]

$$C_{Ta} = 740 \times 22.3\% + 220 \times 77.7\% = 336 \text{ F g}^{-1}$$

b) PANI/RGO composite in this work:

$$C_{Tb} = 740 \times 50\% + 220 \times 50\% = 480 \text{ F g}^{-1}$$

c) HAOANIs:

$$C_{T1} = \frac{2 \times 96485}{0.8 \times 110} = 2193 \text{ F g}^{-1}$$

$$C_{T2} = \frac{2 \times 96485}{0.8 \times 200} = 1206 \text{ F g}^{-1}$$

$$C_{T3} = \frac{4 \times 96485}{0.8 \times 288} = 1675 \text{ F g}^{-1}$$

d) PANI/RGO composite in this work when HAOANIs are generated.

$$C_{Td} = 220 \times 50\% + 1207.5 \times 50\% = 714 \text{ F g}^{-1}$$

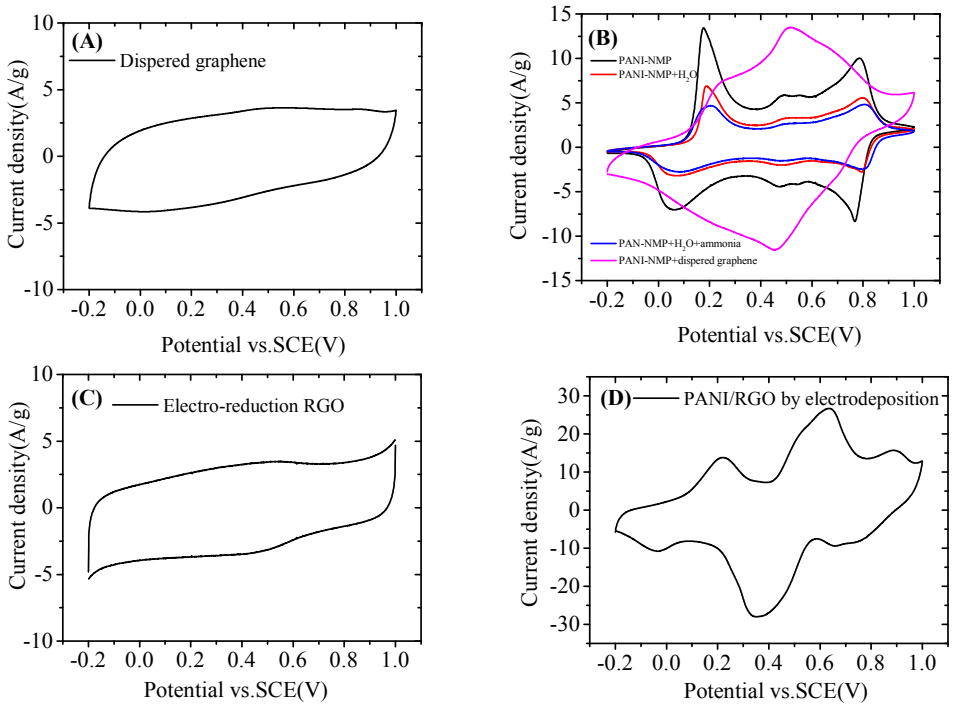

Fig. S1 (A) The CV curves of dispersed graphene.[7] (B) PANI mixed with dispersed graphene. (C) RGO by electrochemical reduction. (D) PANI/RGO by electrodeposition.[8]

Table S1 Comparison of position of the new pair of peaks and capacitances based on graphene-PANI materials

Materials	**Position of new pair of peaks**	**Capacitance**	**Cycle life**	**Ref**
Phase–Separated polyaniline/Graphene Composite	Around 0.4 ~ 0.5V	791 F g^{-1} at 1.14 A g^{-1}	81.1% after 10000 galvanostatic charge–discharge cycles	9
RGO/PANI/RGO paper	Around 0.4 ~ 0.5V	581 F g^{-1} at 1 A g^{-1}	85% after 10000 galvanostatic charge–discharge cycles	10
PANI–IL–graphene	Around 0.4 ~ 0.5V	662 F g^{-1} at 1.0 A g^{-1}	Less than 7.0% after 5000 charge–discharge cycles at 10 A g^{-1}	11
AT-GO composites	Around 0.4 ~ 0.5V	769 F g^{-1} at 1 A g^{-1}	More than 93 to 96% after 2000 cycles	12
3D rGO–PANI Nanofibers	Around 0.4 ~ 0.5V	921 F g^{-1} at 0.45 A g^{-1}	>100% retention at 10 A g^{-1} for 2000 cycles	13
Graphene/PANI composite film	Around 0.4 ~ 0.5V	640 F g^{-1} at 1 A g^{-1}	90% after 1000 charge/discharge cycles	14
PANI@3DGFs composite	Around 0.4 ~ 0.5V	596.1 F g^{-1} at 0.5 A g^{-1}	70.2% capacitance retention after 5000 cycles	15

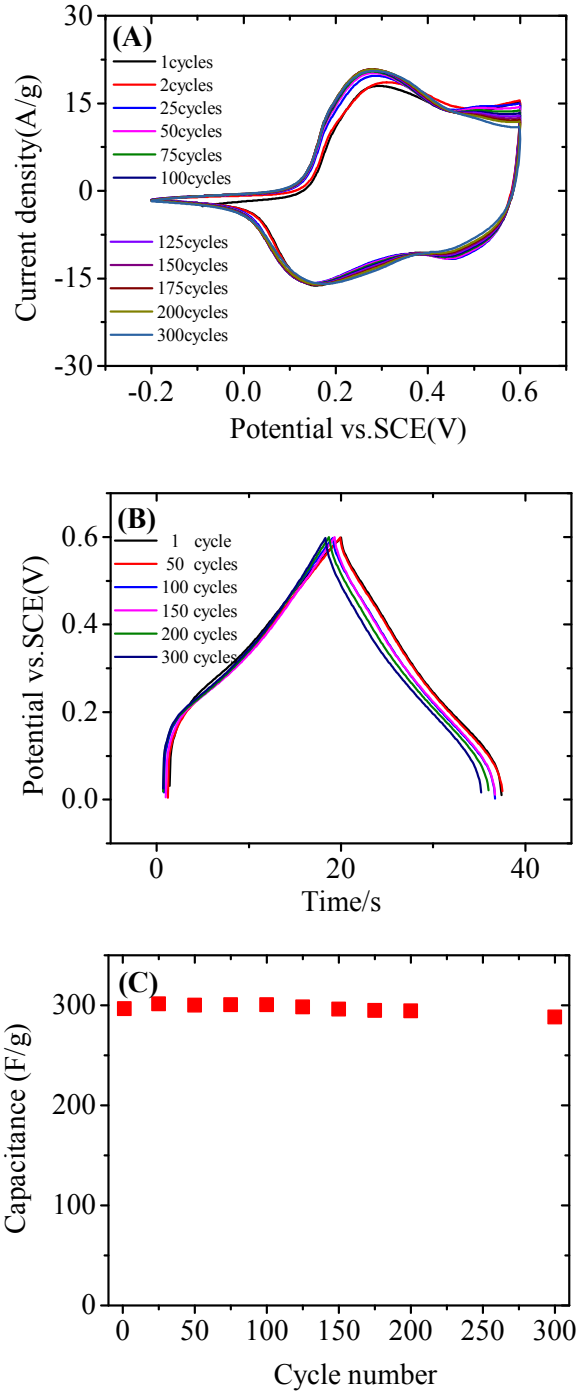

Fig. S2 Capacitive performances of PANI. (A) The CV curves of PANI in the potential ranges from −0.2 ~ 0.6 V at scan rate of 50 $mV \cdot s^{-1}$ within 300 cycles. (B) The corresponding GCD curves. (C) Specific capacitance of PANI at different cycle number.

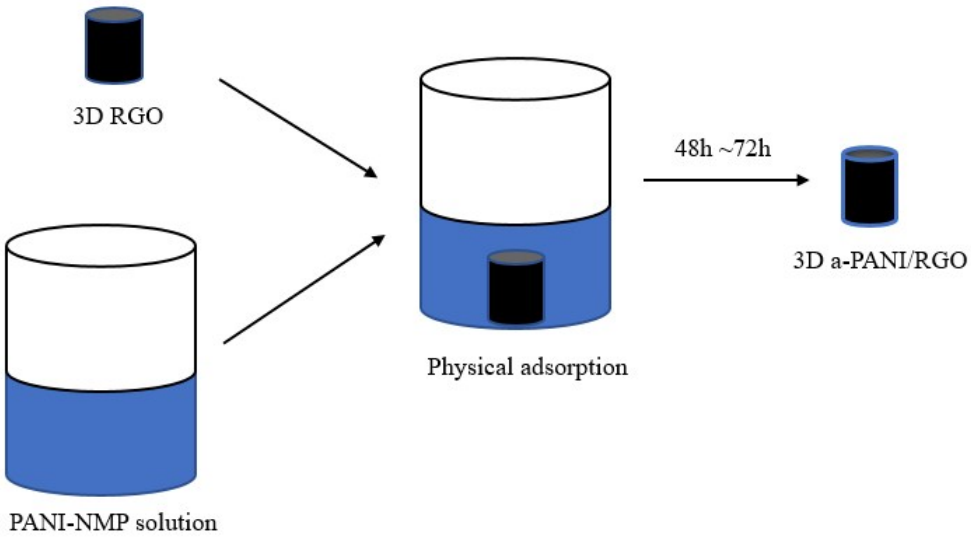

Fig. S3 Schematic diagram of the preparation of 3D a-PANI/RGO composite.

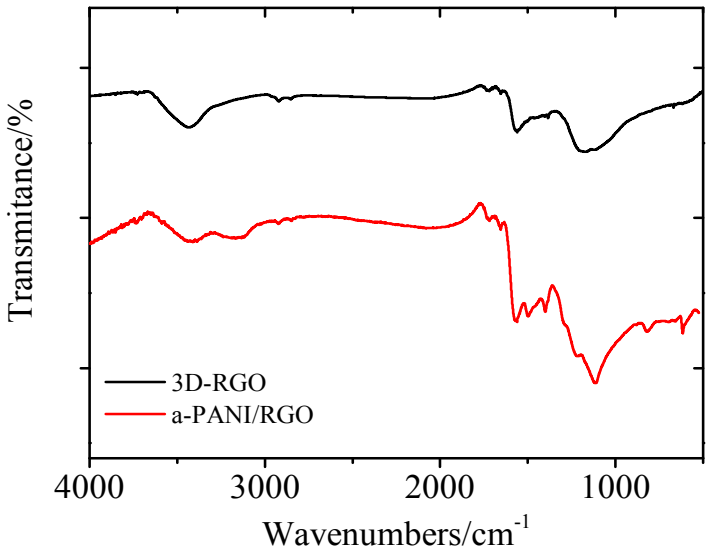

Fig. S4 FT-IR of 3D RGO and a-PANI/RGO composite.

Compared with the FT-IR spectrum of RGO, the new peaks at 1560cm^{-1}, 1490cm^{-1}, 1398cm^{-1}, and 811 cm^{-1} were attributed to the vibrations of –C=N, –C=C, –C–N and –C–H, respectively, which demonstrates the successful combination of PANI with the RGO hydrogel.[16, 17]

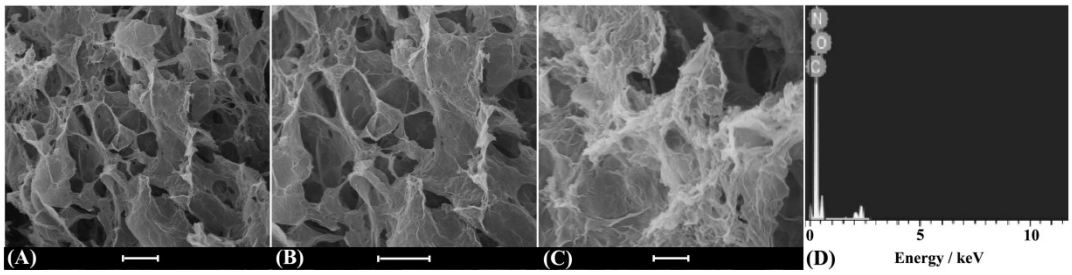

Fig. S5 SEM images of a-PANI/RGO composite. Scale bars: (A) 20μm, (B) 10μm and (C) 5μm. (D) EDX spectrum of a-PANI/RGO composite.

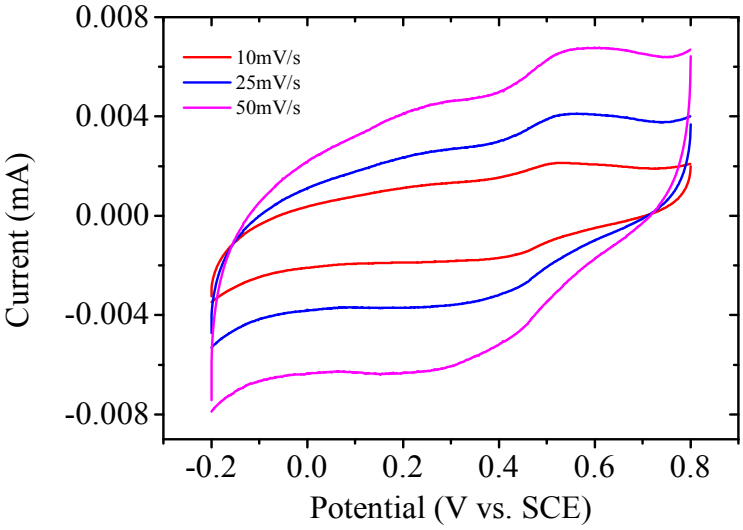

Fig. S6 The CV curves of extraction on GCE at different scan rates.

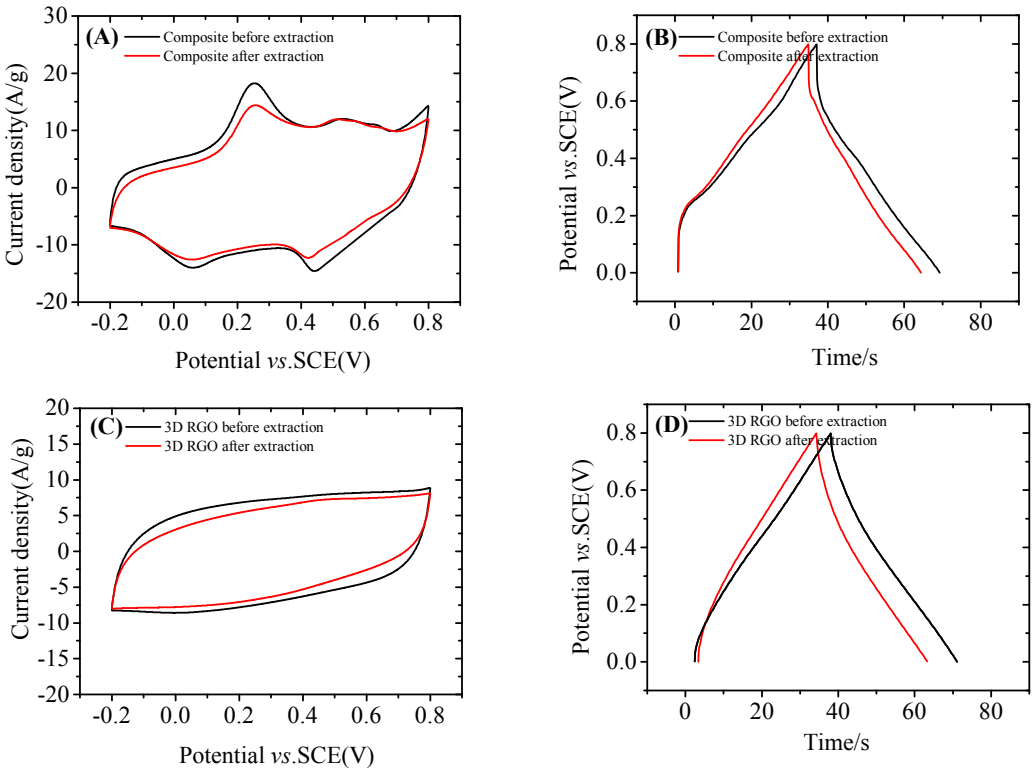

Fig. S7 The CV (A) and GCD (7.8 $A \cdot g^{-1}$) (B) curves of as-prepared 3D a-PANI/RGO composite before and after acetonitrile extraction. The CV (C) and GCD (4.2 $A \cdot g^{-1}$) (D) curves of 3D RGO before and after acetonitrile extraction.

Scheme S1. Degradation of PANI during electrochemical process.

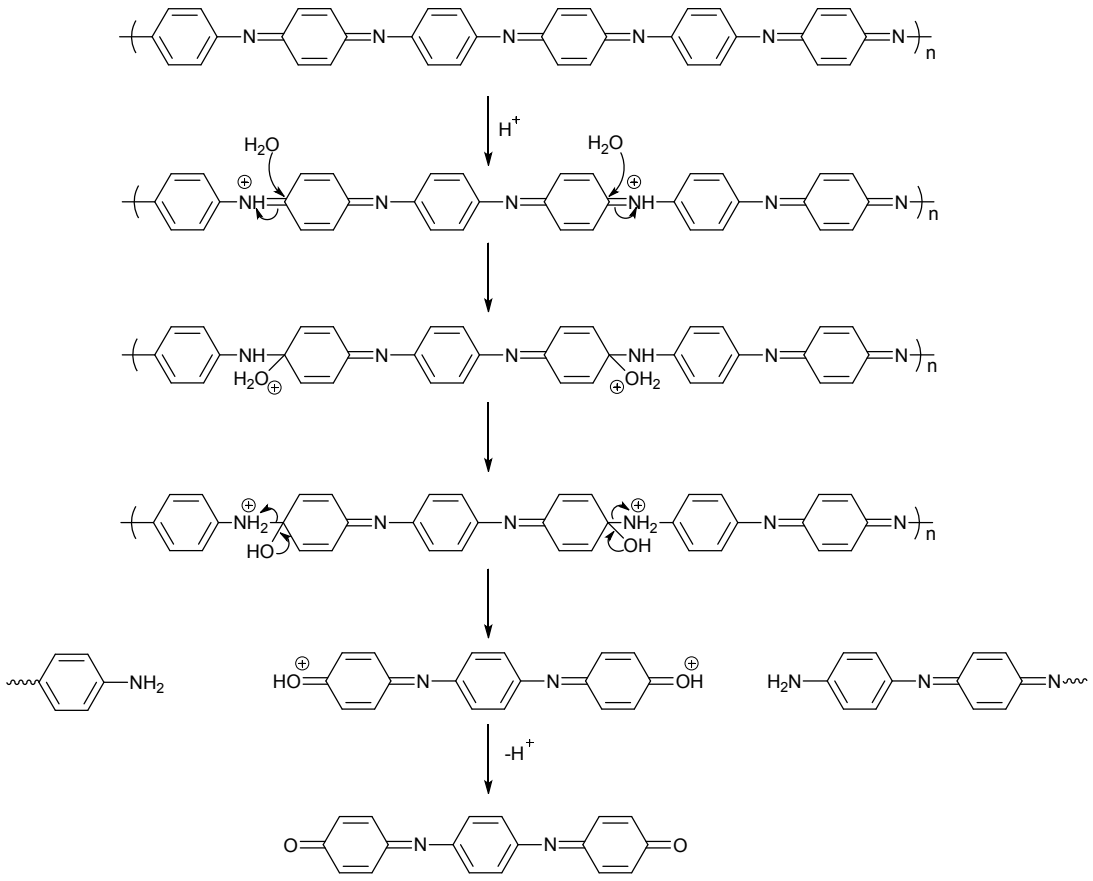

The mechanism of the degradation of PANI under acidic conditions is given above. Compounds containing carbon-nitrogen double bonds can be hydrolyzed to the corresponding aldehydes or ketones.[18, 19] There are plenty of Schiff base structures (Ar-N=C) in oxidized PANI, thus PANI may hydrolysis catalyzed by acid. As shown in Scheme S1, water first adds onto the C=N bond, and then the N group leaves. After deprotonation, C=O bond forms.

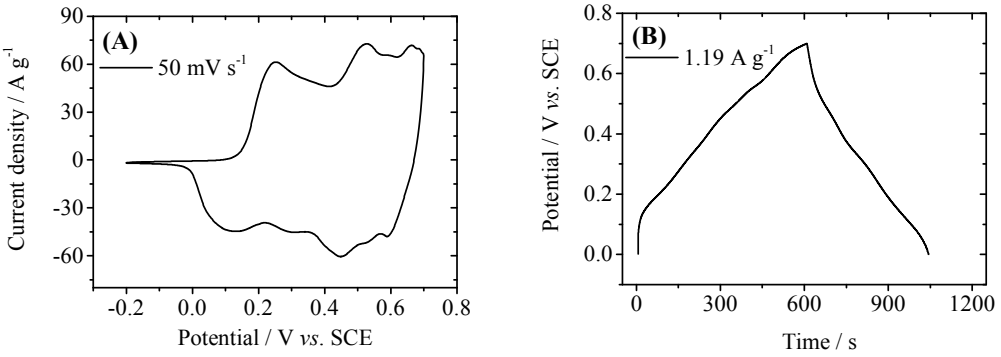

Fig. S8 Electrochemical properties of amino-terminated aniline trimer/PANI composite. (A) CV curve of composite at scan rate of 50 mV s^{-1} in the potential range of − 0.2 ~ 0.7 V. (B) GCD curve of composite at current density of 1.19 $A \cdot g^{-1}$ under the potential of 0 ~ 0.7 V.

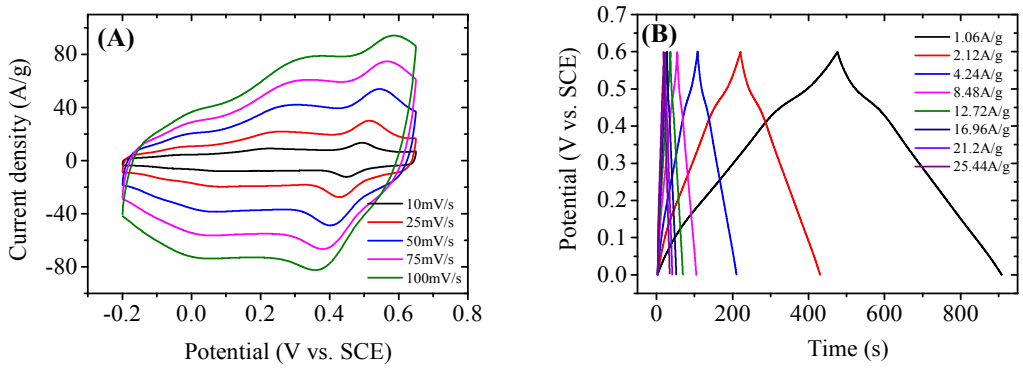

Fig. S9 The different scan rates of CV curves (A) and the specific capacitance at different current density (B).

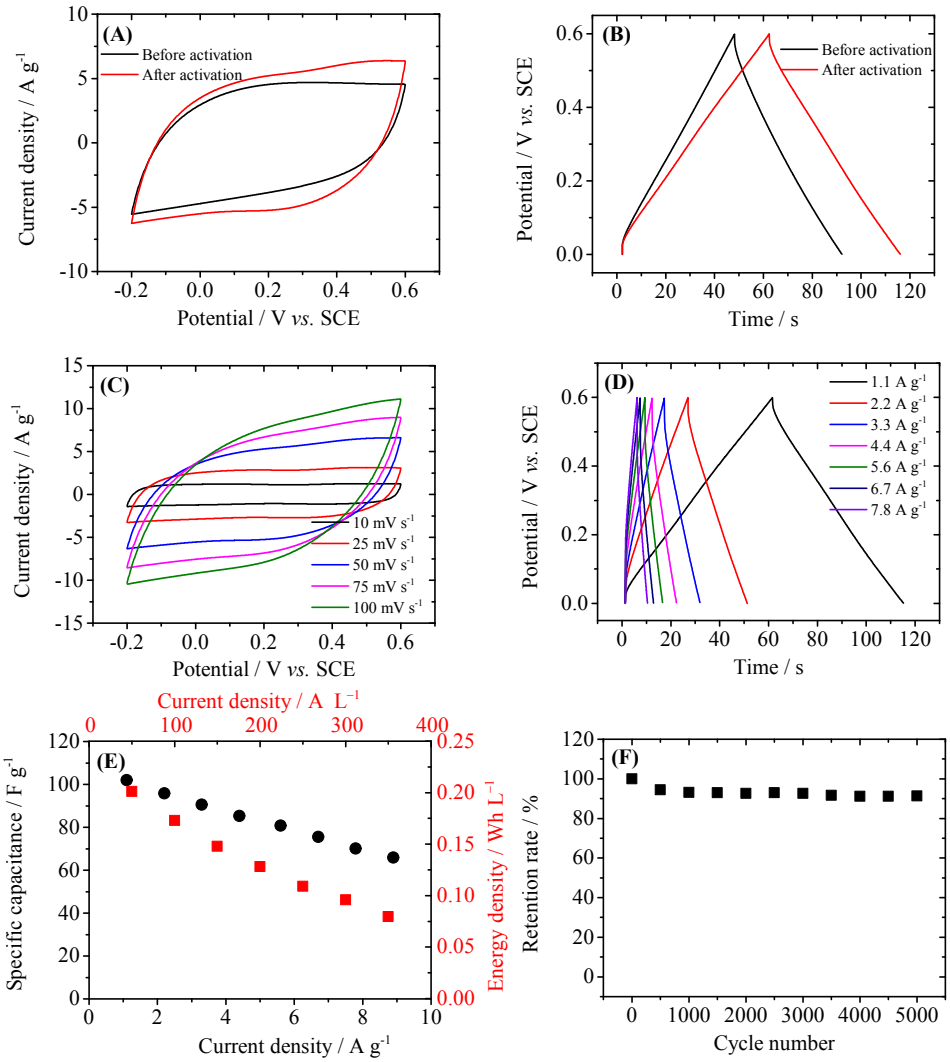

Fig. S10 Capacitive performance of two-electrode devices with PANI/RGO as the anode (mass loading: 5.1 mg cm^{-2}) and pure RGO as the cathode. (A) CV curves of device before and after activation of PANI/RGO at 50 mV s^{-1}. (B) GCD curves of device before and after activation of PANI/RGO at current density of 1.1 $A \cdot g^{-1}$. (C) CV curves of device at different scan rate. (D) GCD curves of device at different current densities. (E) Specific capacitance of device at different current densities. (F) Capacitance retention of device over 5000 cycles at the current density of 7.8 $A \cdot g^{-1}$.

The specific capacitance of the device is calculated from GCD curves:

$$C_{cell} = \frac{I\Delta t}{m(U - IR)}$$

where I is the constant discharge current, Δt is the discharging time, m is the total mass of materials on both electrodes, and U is highest voltage of the cell during charge/discharge process, and IR is the voltage drop upon discharging.

The energy density is calculated using following equation:

$$E_S = \frac{I\int_{discharge} U dt}{V},$$

where V is the total volume of the two electrodes.

Reference

1. C. Peng, X. Zhou, G. Z. Chen, F. Moggia, F. Fages, H. Brisset and J. Roncali, *Chem. Commun.*, 2008, 6606-6608.
2. C. Peng, D. Hu and G. Z. Chen, *Chem. Commun.*, 2011, **47**, 4105-4107.
3. Y. Xu, Z. Lin, X. Zhong, X. Huang, N. O. Weiss, Y. Huang and X. Duan, *Nat. Commun.*, 2014, **5**, 4554.
4. Y. Zhu, S. Murali, W. Cai, X. Li, J. W. Suk, J. R. Potts and R. S. Ruoff, *Adv. Mater.*, 2010, **22**, 3906-3924.
5. L. Zhang and G. Shi, *J. Phys. Chem. C*, 2011, **115**, 17206-17212.
6. H.-P. Cong, X.-C. Ren, P. Wang and S.-H. Yu, *Energy Environ. Sci.*, 2013, **6**, 1185-1191.
7. D. Li, M. B. Muller, S. Gilje, R. B. Kaner and G. G. Wallace, *Nat. Nano*, 2008, **3**, 101-105.
8. K. Chen, L. Chen, Y. Chen, H. Bai and L. Li, *J. Mater. Chem.*, 2012, **22**, 20968-20976.
9. J. Wu, Q. e. Zhang, A. a. Zhou, Z. Huang, H. Bai and L. Li, *Adv. Mater.*, 2016, **28**, 10211-10216.
10. F. Xiao, S. Yang, Z. Zhang, H. Liu, J. Xiao, L. Wan, J. Luo, S. Wang and Y. Liu, *Sci. Rep.*, 2015, **5**, 9359.
11. K. Halab Shaeli Iessa, Y. Zhang, G. Zhang, F. Xiao and S. Wang, *J. Power Sources*, 2016, **302**, 92-97.
12. J. Yan, L. Yang, M. Cui, X. Wang, K. J. Chee, V. C. Nguyen, V. Kumar, A. Sumboja, M. Wang and P. S. Lee, *Adv. Eng. Mater.*, 2014, **4**, 1400781-n/a.
13. N. Hu, L. Zhang, C. Yang, J. Zhao, Z. Yang, H. Wei, H. Liao, Z. Feng, A. Fisher, Y. Zhang and Z. J. Xu, *Sci. Rep.*, 2016, **6**, 19777.
14. X.-M. Feng, R.-M. Li, Y.-W. Ma, R.-F. Chen, N.-E. Shi, Q.-L. Fan and W. Huang, *Adv. Funct. Mater.*, 2011, **21**, 2989-2996.
15. M. Yu, Y. Huang, C. Li, Y. Zeng, W. Wang, Y. Li, P. Fang, X. Lu and Y. Tong, *Adv. Funct. Mater.*, 2015, **25**, 324-330.
16. L. Wang, Y. Ye, X. Lu, Z. Wen, Z. Li, H. Hou and Y. Song, *Sci. Rep.*, 2013, **3**, 3568.
17. Y. Meng, K. Wang, Y. Zhang and Z. Wei, *Adv. Mater.*, 2013, **25**, 6985-6990.
18. A. R. Hajipour, S. Khoee and A. E. Ruoho, *Org. Prep. Proced. Int.*, 2003, **35**, 527-581.
19. S. Hammerum and T. I. Sølling, *J. Am. Chem. Soc.*, 1999, **121**, 6002-6009.